Excitons in solid C_{60}

Eric L. Shirley
National Institute of Standards and Technology, Physics Laboratory, Optical Technology Division, Gaithersburg, Maryland 20899

Lorin X. Benedict and Steven G. Louie
Department of Physics, University of California at Berkeley, Berkeley, California 94720
and Materials Science Division, Lawrence Berkeley Laboratory, Berkeley, California 94720
(Received 6 October 1995; revised manuscript received 30 May 1996)

Exciton levels in undoped, solid C_{60} are calculated using a model Hamiltonian. We find excitation energies of 1.58 and 1.30 eV for the lowest singlet and triplet exciton, respectively, in comparison with the measured energies of 1.83 and 1.55 eV. Singlet and triplet states have similar energy diagrams, wherein exciton states having T_{2g}, T_{1g}, G_g, and H_g symmetries are separated by up to several tenths of an electron volt. As a function of crystal momentum, exciton energies exhibit dispersion from 20 to 40 meV. Theoretical pressure derivatives of exciton energies are presented. [S0163-1829(96)02440-X]

I. INTRODUCTION

For reasons ranging from its geometrical elegance[1] to its role in several intermediate-temperature superconductors,[2] the C_{60} molecule has been subjected to intense scientific scrutiny. Undoped, solid C_{60}, or *fullerite*, is also of fundamental interest because this material serves as a prototypical molecular solid. High sample quality now permits reproducible spectroscopic measurements of many of this substance's properties. In general, molecular solids can be fascinating because their properties reflect both the properties of individual molecules and extended systems. Fullerite is no exception to this rule.

Electronic properties of fullerite that have been studied include electron quasiparticle states and exciton levels. As both measured and predicted, electron densities of states and energy-momentum dispersion relations derive primarily from a molecular level scheme, with level spacings of 1–2 eV. The levels are broadened by intermolecular hybridization of the molecular orbitals (MO's), producing weak banding effects, with bandwidths around 1 eV. Electron states in fullerite are discussed further in Refs. 3–9.

In this work, we present calculations modeling low-lying exciton levels in fullerite. Our approach makes no assumptions regarding the symmetries or character (Frenkel, charge-transfer, or Wannier) of excitons. Instead, we seek an *ab initio* determination of these properties, which depend on the dynamics of a hole in the highest occupied molecular-orbital (HOMO) states and an electron in the lowest unoccupied molecular-orbital (LUMO) states and on a screened electron-hole interaction.

We find the energy needed to form the lowest, optically accessible (i.e., singlet) exciton is 1.58 eV, in reasonable agreement with the measured 1.83 eV.[5] The lowest several exciton levels have strong Frenkel character. The main effects influencing these levels' energies are the average HOMO-LUMO splitting, which equals the minimum quasiparticle gap plus the mean bandwidths for the HOMO- and LUMO-derived bands, and the intramolecular electron-hole attraction, which is dominated by a large monopolar part. Multipolar components of this attraction induce splittings by several tenths of an electron volt between exciton states having predominantly T_{2g}, T_{1g}, G_g, and H_g total symmetries. (In the solid, unlike the molecule, such symmetries are not completely realized. However, for the Frenkel excitons, these symmetries are almost realized, so that the symmetry labels are still descriptive.) Within each group of excitons, e.g., T_{2g} excitons, we find exciton bandwidths ranging from 20 to 40 meV for the low-temperature $Pa3$ structure. The level schemes for triplet and singlet excitons are qualitatively similar. The interval between the lowest triplet and singlet exciton levels is found to be 0.28 eV, in agreement with the 0.28 eV found experimentally.[6] At energies immediately above the Frenkel exciton levels, we find some well-defined charge-transfer exciton states that are energetically close to the quasiparticle, electron-hole continuum.

In the remainder of this article, we describe the present approach used to model excitons and present results for singlet and triplet excitons in the $Fm3$ and $Pa3$ crystals. We illustrate the two kinds of excitons found in this work (Frenkel and charge-transfer), and we present an estimate of pressure derivatives for excitons in $Pa3$ C_{60}. Several pertinent implications and aspects of the results are discussed, and we provide some conclusions.

II. METHODOLOGY

The exciton states are solutions of a Hamiltonian $H_{\rm ex}$. This Hamiltonian consists of three terms, which respectively account for the dynamics of an electron ($H_{\rm el}$) or of a hole ($H_{\rm hole}$), and for the electron-hole interaction ($H_{e\text{-}h}$):

$$H_{\rm ex}=H_{\rm el}+H_{\rm hole}+H_{e\text{-}h}\,.$$

Individually, $H_{\rm el}$ and $H_{\rm hole}$ would govern the dynamics of independent quasiparticles: a single conduction-band electron or valence-band hole in a fullerite crystal. These dynamics are described using a Slater-Koster parametrization of *ab initio* quasiparticle results, presented earlier.[7] Specifically, one has

$$H_{\rm el}=\sum_{\mathbf{R},i}\left(\epsilon_e a^{\dagger}_{\mathbf{R}i}a_{\mathbf{R}i}+\sum_{\mathbf{R}',i'}(t_e^{\mathbf{R}-\mathbf{R}'})_{i,i'}a^{\dagger}_{\mathbf{R}i}a_{\mathbf{R}'i'}\right),$$

where $\mathbf{R}$ and $\mathbf{R}'$ indicate unit cells of the crystal and i and i' indicate T_{1u} (LUMO) orbitals of the various molecules in each unit cell. Indices i and i' also include spin degrees of freedom. Here ϵ_e is the T_{1u} term energy. The t's are transfer (or hopping) integrals between MO's on neighboring molecules, so these are nonzero only when $\mathbf{R}$ and $\mathbf{R}'$ are close. We neglect nonorthogonality of MO's on different molecules. The operators $a^{\dagger}$ and a are the electron creation and annihilation operators for the various MO's. Analogously, for holes we have

$$H_{\rm hole}=\sum_{\mathbf{R},i}\left(\epsilon_h b^{\dagger}_{\mathbf{R}i}b_{\mathbf{R}i}+\sum_{\mathbf{R}',i'}(t_h^{\mathbf{R}-\mathbf{R}'})_{i,i'}b^{\dagger}_{\mathbf{R}i}b_{\mathbf{R}'i'}\right).$$

Based on quasiparticle calculations, the average HOMO-LUMO splitting ϵ_e-ϵ_h is about 3.03 eV in fullerite, whereas the measured value of this quantity ranges from 3.5 eV (Ref. 8) to 3.7 eV.[9] We use the theoretical value of 3.03 eV in the present analysis.

Because of the complexity of the electron-hole interaction, we describe it in four stages. First, we consider the various parts of the electron-hole interaction. Second and third, we discuss interactions when the electron and hole are on different molecules and when the electron and hole are on the same molecule, respectively. Fourth, we discuss effects on the electron-hole interaction because of solid-state screening effects, i.e., the polarizability of the lattice of C_{60} molecules in the crystal. After discussing the form of the electron-hole interaction, we briefly mention how the exciton Hamiltonian is solved.

Our notation is defined as follows. Electron and hole motion are coupled by $H_{e\text{-}h}$, which we write as

$$H_{e\text{-}h}=H^{(1)}_{e\text{-}h}+H^{(2)}_{e\text{-}h},$$

where

$$H^{(1)}_{e\text{-}h}=\sum_{\mathbf{R},i}\sum_{\mathbf{S},j}[(1-\delta_{\tau_{\mathbf{R}i},\tau_{\mathbf{S}j}})W(\tau_{\mathbf{R}i}-\tau_{\mathbf{S}j})a^{\dagger}_{\mathbf{R}i}b^{\dagger}_{\mathbf{S}j}b_{\mathbf{S}j}a_{\mathbf{R}i}]$$

and

$$H^{(2)}_{e\text{-}h}=\sum_{\mathbf{R},i}\sum_{\mathbf{S},j}\left(\delta_{\tau_{\mathbf{R}i},\tau_{\mathbf{S}j}}\sum_{i',j'}\xi_{ii',jj'}a^{\dagger}_{\mathbf{R}i}b^{\dagger}_{\mathbf{S}j}b_{\mathbf{S}j'}a_{\mathbf{R}i'}\right).$$

Here $\tau_{\mathbf{R}i}$ denotes the location of the molecule associated with the ith T_{1u} MO in the $\mathbf{R}$th unit cell; there is a corresponding definition for $\tau_{\mathbf{S}j}$ that involves the H_u MO's. Ostensibly, this division of $H_{e\text{-}h}$ into $H^{(2)}_{e\text{-}h}$ and $H^{(1)}_{e\text{-}h}$ is a division into effects occurring when the electron and hole are on the same and different molecules, respectively.

A different conceptual subdivision of the electron-hole interaction is also worth noting. The interaction may be divided into ''direct'' and ''exchange'' parts.[10] This distinction is important, because one must carefully consider how each part is to be screened. In this work, $H_{\rm ex}$ is really an effective Hamiltonian describing the low-lying excitons formed by $H_u\rightarrow T_{1u}$ electron promotions. All virtual promotions besides $H_u\rightarrow T_{1u}$ ones serve to renormalize the properties of the H_u hole and T_{1u} electron and lead to an *effective electron-hole interaction* that is reflected in $H_{\rm ex}$. In the C_{60} molecule, whether in the vapor phase or solid state, care must be taken to include the effects of these many other, possible promotions: only *these* promotions are treated collectively in screening the exchange *effective* electron-hole interactions, whereas *all* promotions are treated collectively in screening of the direct *effective* interactions.

This particular screening of the exchange parts would not be appropriate in treatments of excited states of molecules and solids involving strictly the full Hamiltonians with bare electrons and holes.[10,11] Yet, as described above, we use an effective Hamiltonian that treats only the dynamics of the T_{1u} electron and H_u hole with an effective fundamental interaction that is screened by the remainder of the system.

Our screening of the exchange parts is not novel. It is highly analogous to a similar screening of the effective fundamental interaction between valence electrons within the core-polarization-potential fashion of core-valence partitioning[12] (as well as analogous to the screening of the fundamental interaction between π electrons when σ and π electrons have been similarly partitioned). As was explicitly derived within the core-polarization-potential framework, for instance, evaluation of the dielectric response of a semiconductor using the random-phase approximation resulted in a screening, because of core-polarization effects, of the exchange part of the (valence) electron- (valence) hole interaction.[12] [To clarify this (standard) terminology, we note that only the exchange part of the electron-hole interaction is included within the random-phase approximation.]

A. Intermolecular electron-hole interactions

Consider the case when $\tau_{\mathbf{R}i}$ and $\tau_{\mathbf{S}j}$ correspond to different molecules. Then for the *screened interaction W* we include effects based on the monopole moments of the T_{1u} or H_u probability distributions on each molecule. This screened interaction includes a term equal to $-e^2/[4\pi\epsilon_0|\tau_{\mathbf{R}i}-\tau_{\mathbf{S}j}|]$, plus a term accounting for solid-state screening effects, which will be described below. Clearly, our $H^{(1)}_{e\text{-}h}$ affects only the direct part of the electron-hole interaction because of the minimal spatial overlaps between orbitals on different molecules.

One might also consider multipolar contributions to intermolecular Coulomb integrals. Such effects could influence exciton bandwidths. However, we presume that such effects are quite small and do not consider them further. In our model, therefore, exciton bandwidths are determined by single-particle hopping through $H_{\rm el}$ and $H_{\rm hole}$. A Frenkel exciton can move from one molecule to its neighbor via successive hops of the electron and hole.

B. Intramolecular electron-hole interactions

If $\tau_{\mathbf{R}i}$ and $\tau_{\mathbf{S}j}$ correspond to the same molecule, we compute the electron-hole interaction as follows. We have

$$\xi_{ii',jj'}=\delta_{ii'}\delta_{jj'}\left[\Phi_0-A\left(\frac{e^2}{4\pi\epsilon_0 R_0}\right)\right]+A\zeta^{D}_{ii',jj'}+A'\zeta^{X}_{ii',jj'}.$$

The term Φ_0 accounts for the solid-state screening effects that occur when the electron and hole are on the same mol-

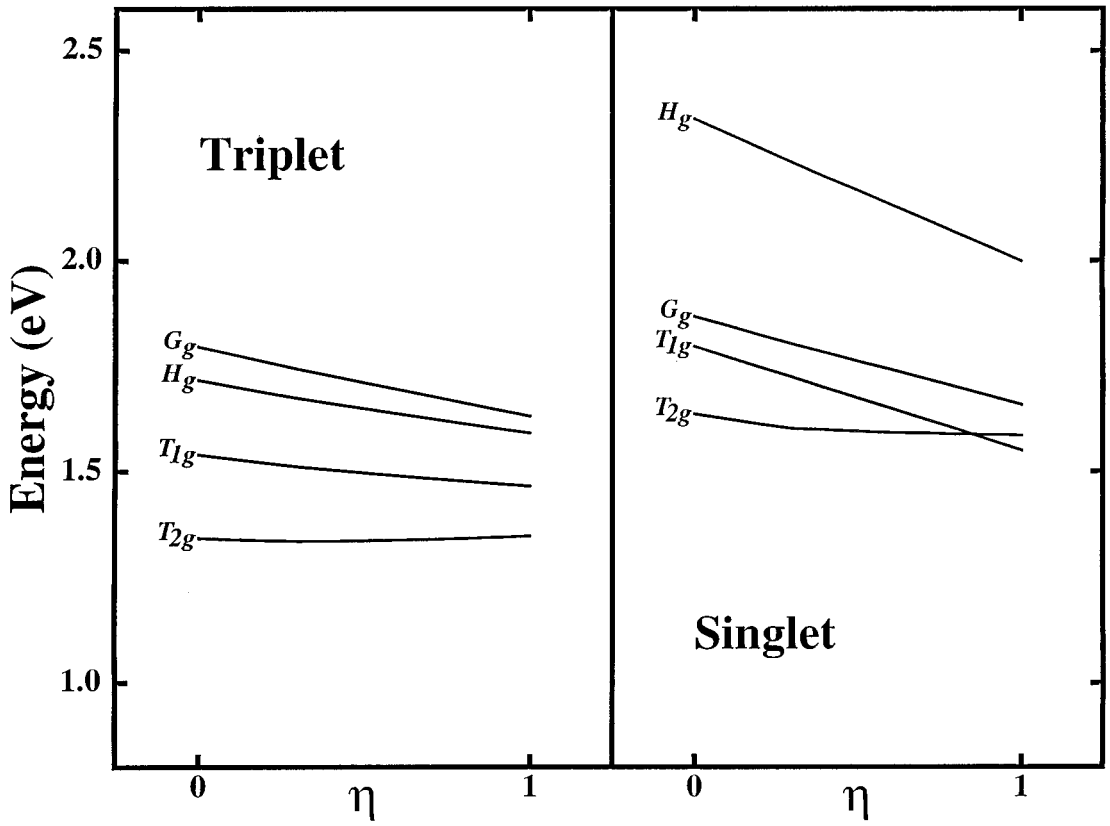

FIG. 1. Approximate dependence of approximate singlet and triplet level schemes (for crystal momentum $\mathbf{q}=0$ in the $Pa3$ structure) on the Parr-Pariser-Pople parameters used for π-electron multicenter integrals. The parameter η defines the admixture of Löwdin and semiempirical (cf. Ref. 13) parameters used in weighted average of these two sets, where Löwdin's parameters have weight $1-\eta$, and the others, weight η. Exciton symmetries are indicated, and splittings within each complex (e.g., T_{2g}) are suppressed in the presentation, to clarify the dependence of results on the parameters.

ecule. The parts scaled by the factor A represent monopole (in brackets) and multipole (outside of brackets) contributions to the intramolecular, direct electron-hole interaction. The parts scaled by the factor A' represent multipole parts of the intramolecular, exchange electron-hole interaction. Modulo scalings by A or A', intramolecular interactions are computed within the Parr-Pariser-Pople approach,[13] which involves a parametrization of multicenter Coulomb integrals for π-electron systems. Reference 13 presents several sets of parameters appropriate for use in calculations with neglect of differential overlap, an assumption made in this work. We use parameters given by Löwdin in this work, whereas a different set of semiempirical parameters gives somewhat different results. To illustrate this, approximate level schemes for triplet and singlet excitons in the $Pa3$ structure are shown in Fig. 1, as we continuously interpolate between Löwdin's and the semiempirical parameters.[13] Notably, the nearly degenerate T_{1g} and T_{2g} singlet levels can change order.

One may be justifiably concerned, *a priori*, with the use of intramolecular electrons, based on studies of benzene, in the study of C_{60}. However, the parameters are fairly independent of the π-electron system studied, in part because the associated Coulomb integrals approach a form of $e^2/[4\pi\epsilon_0 d]$, where d is the distance between two carbon atoms, for $d>0.3$ nm. Therefore, the systematic uncertainty of our extrapolation of parameters from benzene to C_{60} is indicated by the effects in the above comparison of Löwdin's parameters and the semiempirical parameters. To improve precision would require detailed, quantum-chemical treatment of intramolecular correlation effects that are well beyond the scope of this work.

In Fig. 1 and throughout this work, intramolecular direct integrals are scaled by the factor A to achieve the correct interaction as determined from measurements of the lowest triplet state in vapor-phase C_{60}. [Haufler *et al.*[14] found that the lowest triplet state lies 1.7 eV above the molecular ground state in the vapor phase. With an ionization potential 7.6 eV (Ref. 15) and an electron affinity $\simeq$2.6 eV,[16] this implies an electron-hole attraction energy of

$$7.6\ \text{eV}-2.6\ \text{eV}-1.7\ \text{eV}=3.3\ \text{eV}.$$

Without any scaling, the Löwdin parameters would give an attraction energy of 3.98 eV. Therefore, we use $A=0.83$ for those parameters.] Physically, this scaling compensates for the lack of a more complete treatment of intramolecular correlation effects.

Meanwhile, the scaling of the exchange parts of the electron-hole interactions by the factor A' requires further motivation. We cannot have $A=A'$ exactly, because A reflects screening effects via all virtual $H_u\rightarrow T_{1u}$ promotions,

whereas A' should not. Rather, we would expect $A<A'<1$. However, because A is close to 1 and because of the great number of promotions other than those $H_u \rightarrow T_{1u}$ promotions that form excitons, many that are only a few electron volts above the band gap, we expect $A' \approx A$. The validity of such an approximation, which we indeed make, is supported *a posteriori* by the accuracy of our predicted ${}^3T_{2g} \rightarrow {}^1T_{2g}$ interval. Although it is conceptually important that A and A' differ, better knowledge of the latter is not helpful in this system: because variation of A' throughout its possible range would affect the exciton-level energies by a percentage of an electron volt, any uncertainty in A' will contribute minimally to our other systematic uncertainties.

C. Solid-state screening effects

Now let us discuss solid-state screening effects on W in $H_{e\text{-}h}^{(1)}$ and $H_{e\text{-}h}^{(2)}$ and the evaluation of Φ_0. Consider $H_{e\text{-}h}$ acting on a given configuration in which the electron and hole are respectively in some pair of T_{1u} and H_u MO's. There may be multipolar contributions to intramolecular electron-hole interactions. Beyond that, the form of $H_{e\text{-}h}$ implies that its action is otherwise multiplicative: it will not produce a different configuration. This multiplicative action of $H_{e\text{-}h}$ is modified by solid-state screening effects, which are effective screening of the electron-hole interaction via induced molecular dipoles. Each molecule develops a dipole because of the fluctuating electric fields of the electron, the hole, and other molecular dipoles. However, solid-state screening effects are presumably negligible for intramolecular multipolar interactions between the electron and hole.

For computing solid-state screening effects, electric fields of the electron and hole may be approximated by the associated MO's having spherical probability distributions on each molecule. This leads to polarization of molecules in the vicinity of the electron or hole, whereas there is no contribution by a particle to the electric field at the center of a MO's probability distribution. Also, interactions between molecular dipoles are assumed to be adequately treated in a point-dipole picture.[17] We therefore follow this prescription to compute solid-state screening effects. Suppose the electron and hole are located on molecules at positions τ_e and τ_h, while the molecular dipole of a molecule at position τ is indicated by $\mathbf{p}(\tau)$. Then one has

$$\mathbf{p}(\tau)=\frac{\alpha}{4\pi\epsilon_0}\left[\frac{e(\tau_e-\tau)}{|\tau_e-\tau|^3}-\frac{e(\tau_h-\tau)}{|\tau_h-\tau|^3}-\sum_{\tau'}\nabla_\tau[\mathbf{p}(\tau')\cdot\nabla_{\tau'}]\frac{1}{|\tau-\tau'|}\right].$$

Given electron and hole coordinates, all molecular dipoles are determined simultaneously and self-consistently using the above relation. We use the theoretical, static molecular polarizability α and restrict ourselves to linear-response theory. The value of α used, given by Pederson and Quong,[18] includes all intramolecular electron-electron interactions in a reasonable fashion. Computation of solid-state screening effects follows straightforwardly for a finite solid. Application of appropriate boundary conditions permits one to extrapolate these effects to what they would be in an infinite solid or, as is appropriate at a surface, a semi-infinite solid.

The induced dipoles' potential is the sum of a potential induced by the electron and a potential induced by the hole. To obtain solid-state screening effects on the electron-hole interaction, one may include half of the dipoles' potential as ''felt'' by the electron, which would arise because of the hole alone, and half of the dipoles' potential felt by the hole, which would arise because of the electron alone. (These two terms are equal within the model. The electron and hole self-energy effects, i.e., effects of each particle feeling the dipole potentials caused by itself, are already incorporated in the model through $H_{\rm el}$ and $H_{\rm hole}$.)

The solid-state screening effects involve a dynamical screening of the electron-hole interaction: these effects depend on the fluctuating electron and hole coordinates, as opposed to the expectation value of the total, exciton charge distribution. This fact notwithstanding, one needs only to use the static molecular polarizability in the present model, because electron and hole dynamics are slow compared to the dynamics of the relevant, collective electronic molecular excitations. At large $|\tau_e-\tau_h|$, the solid-state screening effects converge to the correct, asymptotic limit, in which the electron-hole interaction is $-e^2/[(4\pi\epsilon_0)\epsilon|\tau_e-\tau_h|]$, where ϵ, the dielectric constant, is related to the molecular polarizability α through the Clausius-Mossotti relation.

D. Solution of the exciton Hamiltonian

We solve $H_{\rm ex}$ with the general form of exciton wave function

$$|\Psi_{n\mathbf{q}}\rangle=\sum_{\mathbf{R}} e^{i\mathbf{q}\cdot\mathbf{R}}\sum_{\mathbf{S}}\sum_{i,j} C_{\mathbf{S};i,j}^{n\mathbf{q}} a_{\mathbf{R}i}^\dagger b_{(\mathbf{R}+S)j}^\dagger|0\rangle.$$

Here the exciton has the total crystal wave vector $\mathbf{q}$, which is a good quantum number in a periodic system; n distinguishes the various exciton states having a given $\mathbf{q}$. Summation of $\mathbf{R}$ over unit cells establishes the crystal wave vector of the exciton, and summation over values of $\mathbf{S}$ permits the hole and electron to be in different unit cells. In practical calculations, we truncate the range of $\mathbf{S}$, and this truncation is progressively relaxed to ensure that each exciton wave function achieves the desired degree of relative electron-hole localization. By summing over i and j, we consider every possible pair of H_u and T_{1u} MO's lying within each pair of unit cells $\mathbf{R}$ and $\mathbf{R}+\mathbf{S}$. Operators $a^\dagger$ and $b^\dagger$ act on the crystal ground-state wave function to create all desired electron-hole pairs states. The C coefficients weigh these pair states according to their amplitudes in the stationary solutions of $H_{\rm ex}$. The solution for singlet or triplet exciton levels may be carried out using preselected combinations of the C coefficients that project onto a given $S-S_z$ subspace. Solving $H_{\rm ex}$, which in this work involves evaluating up to about 10 000 degrees of freedom, is accomplished by iterative diagonalization techniques. Exploiting the sparseness of $H_{\rm ex}$ reduces significantly the required computational resources.

In the setup of $H_{\rm ex}$, one must be careful to include time-reversal effects when describing the hole dynamics, if these dynamics are derived from an electron band structure. Also,

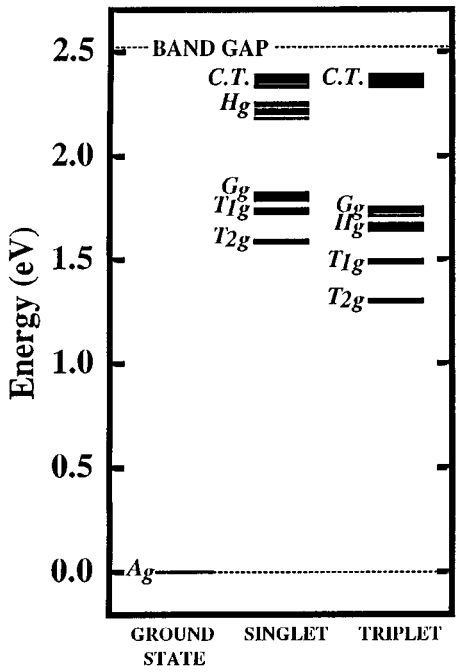

FIG. 2. Level-scheme (for crystal momentum $\mathbf{q}=0$) singlet and triplet excitons in the $Pa3$ structure of C_{60}. Symmetries of Frenkel exciton levels are indicated. Higher-lying, charge-transfer excitons, whose formation requires about 2.33 eV excitation, possess more similar level schemes for singlet and triplet states. The quasiparticle band gap is indicated (at 2.52 eV), although this gap is not necessarily direct in the $Pa3$ structure.

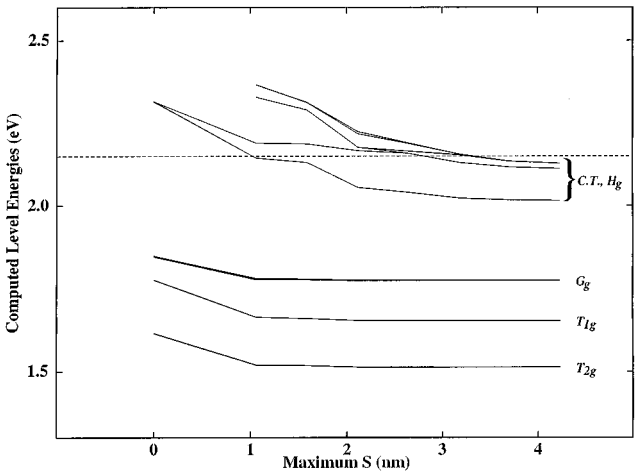

FIG. 3. Dependence of ($\mathbf{q}=\mathbf{0}$) exciton energies, in the $Fm3$ structure, on the maximal range of the wave-function cutoff **S**. As indicated in Table I and as suggested by this plot, only the T_{2g}, T_{1g}, and G_g singlet excitons have nearly complete Frenkel character in the $Fm3$ structure, whereas the H_g excitons acquire considerable charge-transfer character. The horizontal, dashed line indicates the theoretical, $Fm3$ quasiparticle band gap.

one needs to be mindful of possible phase shifts related to **q** when the electron or hole move between adjacent unit cells. Finally, care must be taken regarding effects of Fermi statistics on the signs of $H_{e\text{-}h}$ matrix elements for the singlet- and triplet-exciton cases. Due attention with regard to all of these issues is tedious but straightforward.

III. RESULTS

Except for the results in Fig. 1, all results are based on Löwdin's parameters.[13] In Fig. 2 we present computed level schemes for singlet and triplet excitons in $Pa33$ C_{60}.[19] In the $Fm3$ structure, the lowest exciton levels are typically 0.05 eV lower than those given in Fig. 2. In the $Pa3$ case, the lowest triplet and singlet excitons are formed experimentally with excitations of 1.55 and 1.83 eV, respectively. Here they are predicted in the $Pa3$ case to be formed with 1.30 and 1.58 eV, respectively. The singlet-triplet splitting is therefore accurately predicted. While we find the lowest, singlet-exciton levels have T_{2g} symmetry, the T_{1g} excitons are quite close energetically, and the relative ordering of excitons with these two symmetries depends sensitively on the detailed treatment of the interactions, as discussed previously, and illustrated in Fig. 1. In this regard, one might also compare the various results cited in Ref. 19. Therefore, our results do not establish which symmetry corresponds to that of the lowest-lying singlet exciton. The addenda to the present model, needed to identify the lowest-energy exciton symmetry, are not included in this work.

In Fig. 3 we illustrate the dependence of exciton-level energies on the maximum allowed electron-hole separation. Compared to when the electron and hole are constrained to be on the same molecules, the energies of the actual Frenkel excitons are lowered by 0.1–0.2 eV. This lowering may be estimated by using second-order perturbation theory if we consider as an unperturbed Hamiltonian one that is equal to H_{ex}, but with all transfer integrals reset to zero, and we include effects of the transfer integrals perturbatively. In order of increasing energy, stationary solutions of such a zero-transfer-integral Hamiltonian are excitons with purely Frenkel character, then excitons with purely charge-transfer character, and so forth. Once one includes the true transfer integrals as a perturbation, the energies of Frenkel excitons will be affected by approximately $Z|t|^2/(U-V)$. Here Z is the molecular coordination number and t is a typical transfer-integral magnitude. U and V are the electron-hole interaction when the electron and hole are on the same molecule and on adjacent molecules, respectively. Both U and V are negative and U is larger in magnitude than V.

The above picture of the effects of hopping on exciton energies is qualitatively correct, regarding the 0.1–0.2 eV shifts being discussed. Correspondingly, one would expect exciton bandwidths to be larger in the $Fm3$ crystal than in the $Pa3$ crystal, because transfer integrals (and electron and hole bandwidths) are larger in the former structure. We find this to be the case. For example, the T_{2g} exciton bandwidth is roughly 60 meV in the $Fm3$ structure vs roughly 20 meV in the $Pa3$ structure. We present the exciton bands for the $Pa3$ structure in Fig. 4. (The energies of Frenkel excitons should likewise be lower in the $Fm3$ structure than in the $Pa3$ structure, as has already been noted.)

In Table I we present the relative amounts of Frenkel, charge-transfer, and Wannier character for singlet excitons in the $Fm3$ and $Pa3$ structures. (We define the amount of Frenkel character as the likelihood that the electron and hole are on the same molecule, the amount of charge-transfer

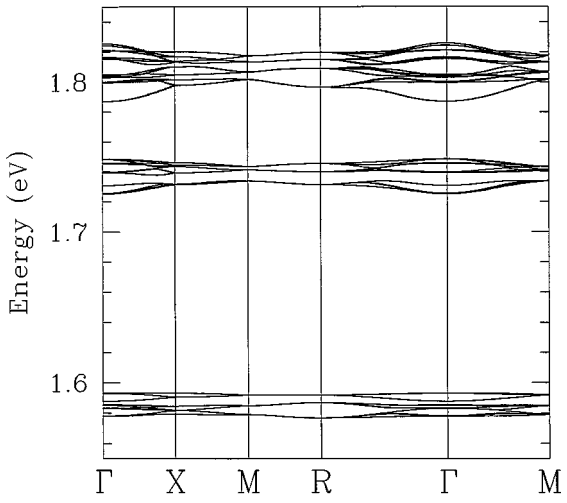

FIG. 4. Exciton energy bands in the $Pa3$ structure of C_{60}. In order of increasing energy, the bands depicted are for singlet excitons with T_{2g}, T_{1g}, and G_g symmetry. In units of $2\pi/a$, where a is the lattice constant, Γ, X, M, and R correspond to crystal momenta (0,0,0), ($\frac{1}{2}$,0,0), ($\frac{1}{2}$,$\frac{1}{2}$,0), and ($\frac{1}{2}$,$\frac{1}{2}$,$\frac{1}{2}$).

character as the likelihood that the electron and hole are on adjacent molecules, and the amount of Wannier character as the likelihood that the electron and hole are even further separated.) The theoretical band gaps are 2.15 and 2.52 eV for the $Fm3$ and $Pa3$ structures, respectively, and strong Frenkel character occurs only for excitons having substantial binding energies. (Binding energy is defined here as the difference between the quasiparticle gap and the energy required to form an exciton.) In Fig. 5 we illustrate the probability distribution for the *relative* electron and hole coordinates for the lowest (Frenkel) singlet-exciton levels and for the 61st (the lowest charge-transfer) singlet exciton level, both results computed in the $Pa3$ structure.

Using the present model, one may also estimate the pressure derivatives of exciton energies. Pressure derivatives arise from the dependence of transfer integrals on the separation between adjacent molecules. Within local-density-functional theory,[20] which reliably estimates the effects of compression on band energies,[21] H_u and T_{1u} bandwidths vary (approximately) inversely with the third power of the molecular volume.[22] Therefore, the effects of intermolecular hopping on exciton energies should vary inversely as the sixth power of the molecular volume, since such effects vary as the squares of the transfer integrals. If one takes the bulk modulus of solid C_{60} to be 10.3 GPa,[23] the model predicts that the pressure derivatives for T_{2g}, T_{1g}, and G_g exciton energies are -44, -44, and -54 meV/GPa in the $Pa3$ structure, respectively. This is in reasonable agreement with the observed pressure derivatives, -45 ± 5, -60 ± 8, and -80 ± 10 meV/GPa of three spectral features near the absorption edge of the $Pa3$ structure.[5]

TABLE I. Relative amounts of Frenkel, charge-transfer, and Wannier character for singlet excitons in $Fm3$ and $Pa3$ crystals. An asterisk denotes that no well-defined trend is identified.

Symmetry	Binding energy (eV)	Molecular character (%)	Charge-transfer character (%)	Wannier character (%)
		$Fm3$ crystal structure		
T_{2g}	0.64	89	10	1
T_{1g}	0.50	87	12	1
G_g	0.38	91	8	1
H_g	*	*	*	*
		$Pa3$ crystal structure		
T_{2g}	0.94	97	3	0
T_{1g}	0.79	96	4	0
G_g	0.73	96	4	0
H_g	0.34	75	23	2
next higher	0.19	1	77	22

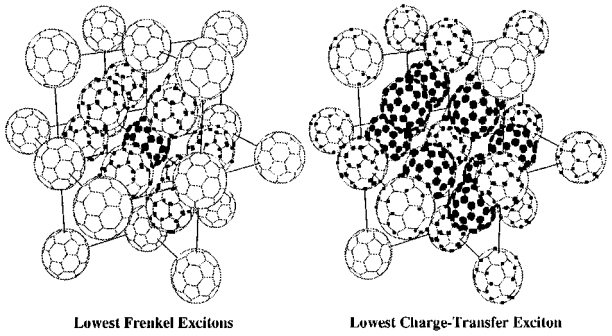

FIG. 5. *Relative* electron-hole coordinates for the T_{2g} and the 61st (lowest charge-transfer) exciton state in the $Pa3$ structure of C_{60} for $\mathbf{q}=0$. Given that the hole is located on the central molecule, the electron probability distribution is presented in scatter-plot fashion. At the same time, the electron and hole move together throughout the crystal with some total crystal momentum, as our model describes. The concentration of the electron probability distribution on atomic sites within each molecule is presented only schematically.

IV. DISCUSSION

A strong Frenkel character of low-lying excitons in the fullerites is suggested by experiments measuring the Zeeman effect[5] and by the remarkable similarity of optical absorption spectra for C_{60} in the solid state and dissolved in *n*-hexane as well as other solutions.[24] Whereas optical spectra primarily probe singlet excitons, we note also the closeness of the 1.55 eV required to form a triplet exciton in the solid in electron, energy-loss experiments and the 1.7 eV required in the vapor phase. Indeed, upon consideration of the nature of the C_{60} molecule and its H_u and T_{1u} MO's, these C_{60} Frenkel excitons are aptly described in the fashion used by Knox[25] regarding Frenkel excitons in other molecular solids. That is, the formation of an exciton does not necessarily imply a substantial alteration in the charge distribution in the solid, but perhaps only a more subtle rearrangement of internal molecular degrees of freedom. On the simplest level, energies required for formation of both triplet and singlet excitons exhibit a 0.1–0.15 eV downward shift in the solid, if

one considers results for isolated C_{60} molecules and C_{60} molecules in the solid state. This sort of redshift is commonly attributed to lowering of energies of nominally Frenkel excitons via acquisition of some charge-transfer character in the solid.

While the difference between quasiparticle results and experiment for the average HOMO-LUMO splitting is from 0.5 to 0.7 eV, we find much closer agreement with experiment regarding the respective energy required to form triplet and singlet excitons, 1.30 and 1.58 eV in theory, vs 1.55 and 1.83 eV in experiment. This suggests that part of the discrepancy between quasiparticle and photoemission results might be intrinsic to the photoemission technique, which is, in fact, a surface-sensitive probe. In particular, the model used to describe solid-state screening effects suggests that a lower molecular coordination number at the surface could give a larger apparent HOMO-LUMO splitting by about 0.25 eV for the topmost layer of a (111)-terminated C_{60} crystal and by 0.14 and 0.12 eV for the next two layers. Furthermore, the present screening model suggests that solid-state screening effects should reduce the HOMO-LUMO splitting by about 1.6 eV from what it would be in the vapor phase. Hence the present results predict that the difference between ionization potential and electron affinity of vapor-phase C_{60} would be roughly 3.0 eV + 1.6 eV = 4.6 eV. This differs by only 0.4 eV from the measured value of 5.0 eV for that difference.

An unresolved issue in this work that we have yet to mention is the role of vibrational effects in measured excitation spectra. Vibrational effects are believed to account for the observed cross sections for creating the lowest-lying, parity-forbidden excitons by optical means, whereas electric-quadrupole effects would produce much smaller cross sections. Vibrational effects also cause absorption spectra to exhibit many more lines than the discrete lines predicted theoretically, which is direct evidence for Herzberg-Teller mechanisms. A more detailed account of optical data for solid C_{60} should also address the possibilities of Jahn-Teller-type mechanisms.

V. CONCLUSION

In summary, we have calculated the properties of excitons in undoped, solid C_{60}. Our model involves a conduction-band T_{1u} electron and a valence-band H_u hole, whose motions are coupled by their mutual attraction. The isolated dynamics of the particles were described previously within a quasiparticle approach. The electron-hole attraction is modeled using a screened Coulomb interaction. Intramolecular electron-hole interactions are described using a semiempirical Parr-Pariser-Pople scheme. These and intermolecular electron-hole interactions are treated in a fashion that accounts for their being effectively screened by the lattice of polarizable molecules.

We predict that the lowest-lying excitons exhibit a strong Frenkel character, whereas some higher-lying excitons exhibit a distinct charge-transfer character. The results for Frenkel excitons are consistent with previous studies dealing with isolated C_{60} molecules.[19] The lowest triplet and singlet excitons are found to have T_{2g} symmetry and can be formed with an excitation energy of 1.30 and 1.58 eV, respectively. These energies differ from the experimentally measured values by 0.25 eV and the singlet-triplet splitting is accurately predicted. In our results, the T_{2g} and T_{1g} singlet excitons lie close in energy, and their ordering is sensitive to the precise Parr-Pople-Pariser parameters used, so this work does not establish which is actually the lowest. Within the singlet and triplet cases, the exciton states characterized by different symmetries (T_{2g}, T_{1g}, G_g, and H_g) span an energy range of several tenths of an electron volt. As a function of crystal momentum, exciton energy levels disperse by about 20 meV in the $Pa3$ structure.

Because the average HOMO-LUMO separation in solid C_{60} is around 3 eV, the intramolecular electron-hole interaction (or electron-hole, ''Hubbard U'' parameter) is about -1.5 eV. Besides the average HOMO-LUMO separation and intramolecular electron-hole attraction, the energies of exciton levels are also influenced by multiplet effects and (very slightly) by banding effects. Just as for the electron quasiparticle states in this molecular solid, we observe a coexistence, in the properties of excitons, of features that are characteristic of single molecules and of extended systems.

ACKNOWLEDGMENTS

E. L. S. acknowledges support of this work, in its initial stages, under the auspices of the U.S. Department of Energy by Lawrence Livermore National Laboratory, under Contract No. W-7405-ENG-48. This work was also funded by NSF Grant No. DMR95-20554 and U.S. DOE under Contract No. DE-AC03-76SF00098. We have benefited from interactions with G. Martinez through the France-Berkeley Fund Program and from discussions with G. A. Sawatzky.

[1] H. W. Kroto *et al.*, Nature (London) **318**, 162 (1985).
[2] A. F. Hebard *et al.*, Nature (London) **350**, 600 (1991).
[3] N. Troullier and J. L. Martins, Phys. Rev. B **46**, 1754 (1992).
[4] J. H. Weaver *et al.*, Phys. Rev. Lett. **66**, 1741 (1991).
[5] C. Hartmann *et al.*, Phys. Rev. B **52**, R5550 (1995).
[6] G. Gensterblum, Phys. Rev. Lett. **67**, 2171 (1991).
[7] E. L. Shirley and S. G. Louie, Phys. Rev. Lett. **71**, 133 (1993); S. G. Louie and E. L. Shirley, J. Phys. Chem. Solids **54**, 1767 (1993).
[8] R. W. Lof *et al.*, Phys. Rev. Lett. **68**, 3924 (1992).
[9] J. H. Weaver, J. Phys. Chem. Solids **53**, 1433 (1992).
[10] L. J. Sham and T. M. Rice, Phys. Rev. **144**, 708 (1966); W. Hanke and L. J. Sham, Phys. Rev. Lett. **43**, 387 (1979); Phys. Rev. B **21**, 4656 (1980).
[11] W. Ekardt and J. M. Pacheco, Phys. Rev. B **52**, 16 864 (1995); G. Onida *et al.*, Phys. Rev. Lett. **75**, 818 (1995).
[12] E. L. Shirley, X. Zhu, and S. G. Louie, Phys. Rev. Lett. **69**, 2955 (1992); E. L. Shirley and R. M. Martin, Phys. Rev. B **47**, 15 413 (1993).
[13] R. G. Parr, *The Quantum Theory of Molecular Electronic Structure* (Benjamin, New York, 1963). The parameters are taken from the last two columns on p. 67. However, with little approximation, we only account for parameters of type $(00|NN)$ and extrapolate the trends followed by these parameters to

longer distances than are found in the benzene molecule. (The parameters approach the form $e^2/[4\pi\epsilon_0 R]$, where R is the separation between two carbons.)

[14] R. E. Haufler *et al.*, Chem. Phys. Lett. **179**, 449 (1991).

[15] J. de Vries *et al.*, Chem. Phys. Lett. **188**, 159 (1992); J. A. Zimmerman, J. R. Eyler, S. B. H. Bach, and S. W. McElvany, J. Chem. Phys. **94**, 3556 (1991); D. L. Lichtenberger *et al.*, Chem. Phys. Lett. **176**, 203 (1991).

[16] L.-S. Wang, J. Conceiao, C. Lin, and R. E. Smalley, Chem. Phys. Lett. **182**, 5 (1991).

[17] An analogous treatment of screening effects is used in Ref. 18.

[18] M. R. Pederson and A. A. Quong, Phys. Rev. B **46**, 13 584 (1992).

[19] For theoretical studies of the C_{60} level scheme in the vapor phase, see F. Negri, G. Orlandi, and F. Zerbetto, Chem. Phys. Lett. **144**, 31 (1988); I. Laszlo and L. Udvardi, J. Mol. Struct. **183**, 271 (1989).

[20] P. Hohenberg and W. Kohn, Phys. Rev. **136**, 864 (1964); W. Kohn and L. J. Sham, *ibid.* **140**, 1133 (1965).

[21] For instance, see H. Chacham, X. Zhu, and S. G. Louie, Phys. Rev. B **46**, 6688 (1992), and references therein.

[22] J. L. Martins and N. Troullier, Phys. Rev. **46**, 1766 (1992); we infer the effects of compression on bandwidths from the results presented in this work.

[23] A. Lundin and B. Sundqvist, Europhys. Lett. **27**, 463 (1994).

[24] For instance, one might compare the similarity of spectral features found in Ref. 5 and in S. Leach *et al.*, Chem. Phys. **160**, 451 (1992); Y. Wang *et al.*, Phys. Rev. B **51**, 4547 (1995).

[25] R. S. Knox, *Solid State Physics, Advances in Research and Applications, Suppl. Vol. 3* (Academic, New York, 1963).